nature ecology & evolution

ARTICLES

PUBLISHED: 22 JUNE 2017 | VOLUME: 1 | ARTICLE NUMBER: 0195

Widely used marine seismic survey air gun operations negatively impact zooplankton

Robert D. McCauley[1]*, Ryan D. Day[2], Kerrie M. Swadling[3], Quinn P. Fitzgibbon[2], Reg A. Watson[2] and Jayson M. Semmens[2]*

Zooplankton underpin the health and productivity of global marine ecosystems. Here we present evidence that suggests seismic surveys cause significant mortality to zooplankton populations. Seismic surveys are used extensively to explore for petroleum resources using intense, low-frequency, acoustic impulse signals. Experimental air gun signal exposure decreased zooplankton abundance when compared with controls, as measured by sonar (~3–4 dB drop within 15–30 min) and net tows (median 64% decrease within 1 h), and caused a two- to threefold increase in dead adult and larval zooplankton. Impacts were observed out to the maximum 1.2 km range sampled, which was more than two orders of magnitude greater than the previously assumed impact range of 10 m. Although no adult krill were present, all larval krill were killed after air gun passage. There is a significant and unacknowledged potential for ocean ecosystem function and productivity to be negatively impacted by present seismic technology.

Phytoplankton and their grazers—zooplankton—underpin ocean productivity[1,2], therefore significant impacts on plankton by anthropogenic sources have enormous implications for ocean ecosystem structure and health. In addition, a significant component of zooplankton communities comprises the larval stages of many commercial fisheries species. Healthy populations of fish, top predators and marine mammals are not possible without viable planktonic productivity[1–3].

Man's dependence on fossil fuels requires continual exploration for new resources. Deposits of undiscovered oil and gas reserves in the world's oceans[4] are estimated to be substantial (Fig. 1), with exploration occurring in most petroleum provinces. In the marine environment, exploration is achieved via an acoustic imaging technique that uses intense, low-frequency impulse signals generated near the sea surface and directed into the seabed ('seismic surveys')[5]. Spatially distributed arrays of air guns simultaneously release high-pressure air (13.8 MPa or 2,000 psi) into the water to produce the impulse signal. Reflections from sub-sea density discontinuities received by strings of hydrophones enable sub-sea image generation. Commonly, a series of closely spaced parallel tracks are followed to systematically survey large swathes of ocean, each track with a series of acoustic signal locations (Fig. 1b,c)[5].

Published details of global seismic survey activity are scarce. As an example of effort, in Australian waters alone during 2014 and early 2015, an average of 15,848 km of petroleum-related marine seismic surveys were completed every three months[6]. Along with petroleum exploration, seismic surveys are also used: (1) to image sub-sea formations likely to be used as 'traps' for sequestering CO_2 (ref. [7]); (2) in scientific surveys of the Earth's geology; 3) (for shallow, engineering-related 'site' surveys; or (4) for monitoring petroleum recovery from producing fields[5].

Our understanding of the impact of seismic surveys on the environment is still developing. Considerable effort has been put into understanding the impacts on whales, with evidence of affected behaviour and hearing physiology[8]. Although fish have received less attention[9], behavioural and pathological impacts have been reported for adults[10–13] and eggs[14,15]. Comparatively little effort has been focussed on impacts on invertebrates[16,17]. One study on larval invertebrates showed significant malformations to scallop veliger larvae from simulated air gun exposure in the laboratory[18], whereas a second found no meaningful impacts on larval hatching success or viability immediately post-hatching for lobster eggs exposed to an air gun *in situ* while on the adult female[19]. No published studies have been conducted on seismic impacts on plankton. On small scales zooplankton can be surprisingly mobile, capable of moving several body lengths per second[20–23]; however, they cannot escape an approaching air gun array. We cannot fully understand impacts of seismic surveys on higher order fauna or on an ecosystem level without knowledge of how organisms at the base of the food chain respond. Our experiments were designed to assess how operation of a single air gun (2.46 l or 150 $inch^3$) of similar mean volume to those used commercially in an array (2.57 l or 157 $inch^3$ from 25 arrays[24]), operating in a field environment, would impact the local zooplankton field. To investigate potential impacts, sonar surveys, net tows for zooplankton abundance and measurements of dead to total zooplankton counts were assessed before and after air gun operations.

Results

Replicated experiments were conducted on the 2 and 3 March 2015 (Day 1 and Day 2; operations shown in Fig. 2 for Day 1). The conductivity–temperature–depth (CTD) casts (Supplementary Fig. 1) suggested that the upper 25 m of the water column was well mixed, so drifter measurements applied to the entire upper water column. At the time of air gun runs, drift rates were 0.19 m s^{-1} at 171° on Day 1 and 0.12 m s^{-1} at 56° on Day 2. Thirty-four plankton taxa were

[1]Centre for Marine Science and Technology, Curtin University, GPO Box U 1987, Perth 6845, Western Australia, Australia. [2]Institute for Marine and Antarctic Studies, Centre for Fisheries and Aquaculture, University Tasmania, Private Bag 49, Hobart, 7001 Tasmania, Australia. [3]Institute for Marine and Antarctic Studies, Centre for Ecology and Biodiversity, Antarctic Climate and Ecosystems Cooperative Research Centre, Private Bag 80, Hobart, 7001 Tasmania, Australia. *e-mail: R.McCauley@cmst.curtin.edu.au; jayson.semmens@utas.edu.au

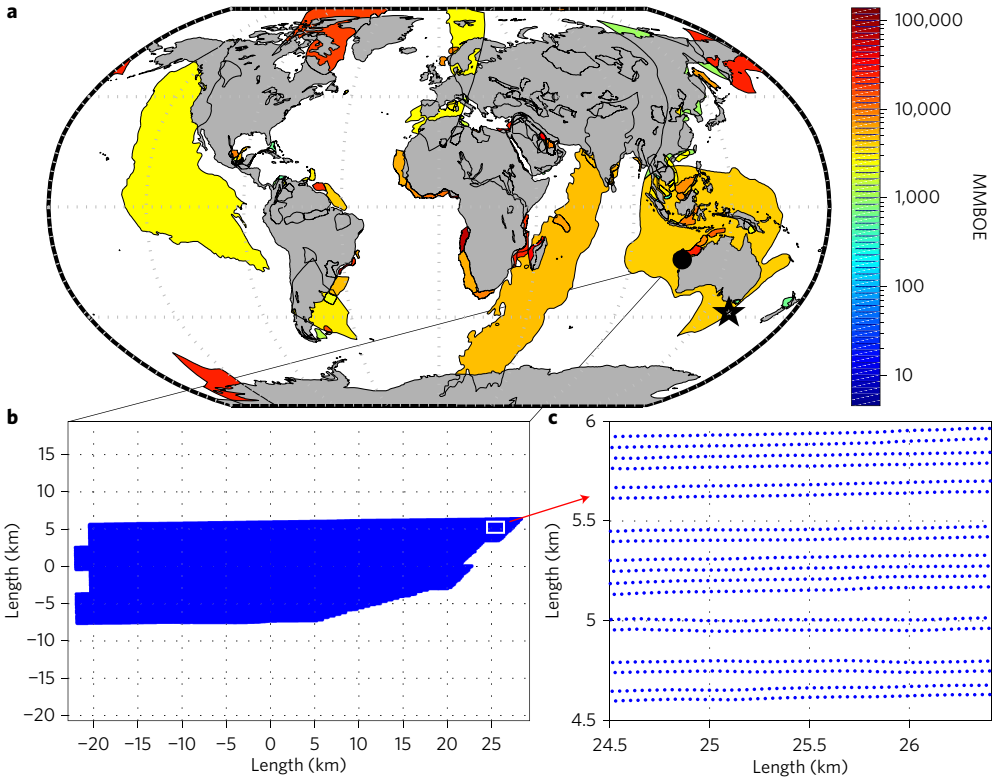

Figure 1 | Potential undiscovered oil deposits worldwide and seismic survey scales. a, Estimated undiscovered marine oil deposits shown by geological province using a logarithmic colour scale in millions of barrels of oil equivalent (MMBOE; source: USGS data[6] for 2012), location of experiment shown by a star symbol. **b**, A typical 3D seismic survey area, located by the black circle in **a**. **c**, Close-up of seismic lines with individual air gun firing locations, from the area indicated by the white rectangle in **b**.

counted in net tows (abundance as individuals (ind.) m^{-3}, listed in Supplementary Table 1). After excluding tows with zero values, 189 taxa/tow combinations ('taxa/tow') were available for comparison of abundance. The taxonomic composition of control tows was similar on Days 1 and 2, with copepods comprising 71% of total taxa counted, cladocerans 15%, euphausiid larvae 4%, appendicularians 5% and the remainder comprising meroplanktonic groups such as larvae of decapods, polychaetes and molluscs. Of the Euphausiidae (krill, *Nyctiphanes australis*), only larval forms were present in samples, possibly due to low net tow speeds. One shark was sighted immediately after the air gun transect on Day 2 and no marine mammal sightings were made.

The site characteristics differed between Days 1 and 2 based on control sonar backscatter observations, zooplankton net tow abundance and locations of fish in the water column. On Day 2, control sonar results showed a significant decrease in zooplankton backscatter (Sv, dB re m^{-3}) from Day 1 ($P << 0.001$, two-tailed t-test when comparing mean values within 6–15 m depth range and 10 m range increments, mean ± s.d. of −81 ± 0.1 and −85 ± 0.1, Days 1 and 2, respectively). On Days 1 and 2, the numbers of individual fish targets per 100 m in the control sonar transects were similar (6.8 and 6.1 fish, respectively), but on Day 2 significantly more of these fish were in the water column rather than close to the seabed (comparing mean fish depth below sea surface Days 1 and 2 in 5–25 m depth range, $P < 0.05$, two-tailed t-test). Sonar-derived fish schools were similar in number and area on Days 1 and 2 (5 and 7 schools of 82 and 106 m^2, respectively). The mean and median zooplankton abundance decreased by 89% and 96%, respectively (Fig. 3d), when comparing ratios of control zooplankton abundance (Day 2/Day 1) using all taxa/tows with non-zero data ($N = 78$), with data highly skewed to lower abundances in any tow made on Day 2. Mean control abundance had decreased by 91% on Day 2 with all taxa combined each day ($N = 30$).

When comparing exposed with control zooplankton abundance for Days 1 and 2 (Supplementary Table 1), 58% of taxa abundance (ind. m^{-3}) were reduced by ≥50% after air gun exposure when using all taxa pooled for all range categories (so excluding range effects) and only taxa with >10 counts in exposed or control groups ($N = 48$). Furthermore, there was a statistically significant lower zooplankton abundance after air gun exposure ($P < 0.001$, two-tailed t-test) when comparing ratios of control abundance with exposed divided by mean control ratios (exposed/control), using all taxa combined or using all crustacean taxa. The distribution of exposed/control abundance for all taxa was skewed to low values with a median abundance reduction of 64%, and 37% with an abundance decrease of ≥95%. For exposed/control ratios ≥1, or no impact, 89% of these occurred on Day 2 when total zooplankton abundance was lower, and 50% of these occurred on Day 2 at the greatest range from the air gun signal (1,200–1,300 m). Exposed abundance reductions of no-change (0%), 25% and 50% compared with control values occurred at ranges of 808, 639 and 409 m, respectively (s.d. 390, 312, 270 m, respectively), as calculated from means of fitted power curves of abundance reduction with range from the drift translated air gun signal location (DTASL; see Supplementary Table 2 for plankton tow ranges, Methods for DTASL definition) for ten independent taxa with r^2 value of >0.8 where only tows with $N > 10$ (control or exposed) were used to generate the curves. Copepods and cladocerans comprised 86% of total zooplankton present, so their pooled abundance reduction with range after air gun passage is important (Fig. 3e). The ranges at which, respectively, no change, and abundance reductions of 25% and 50% occurred for copepods and cladocerans, were

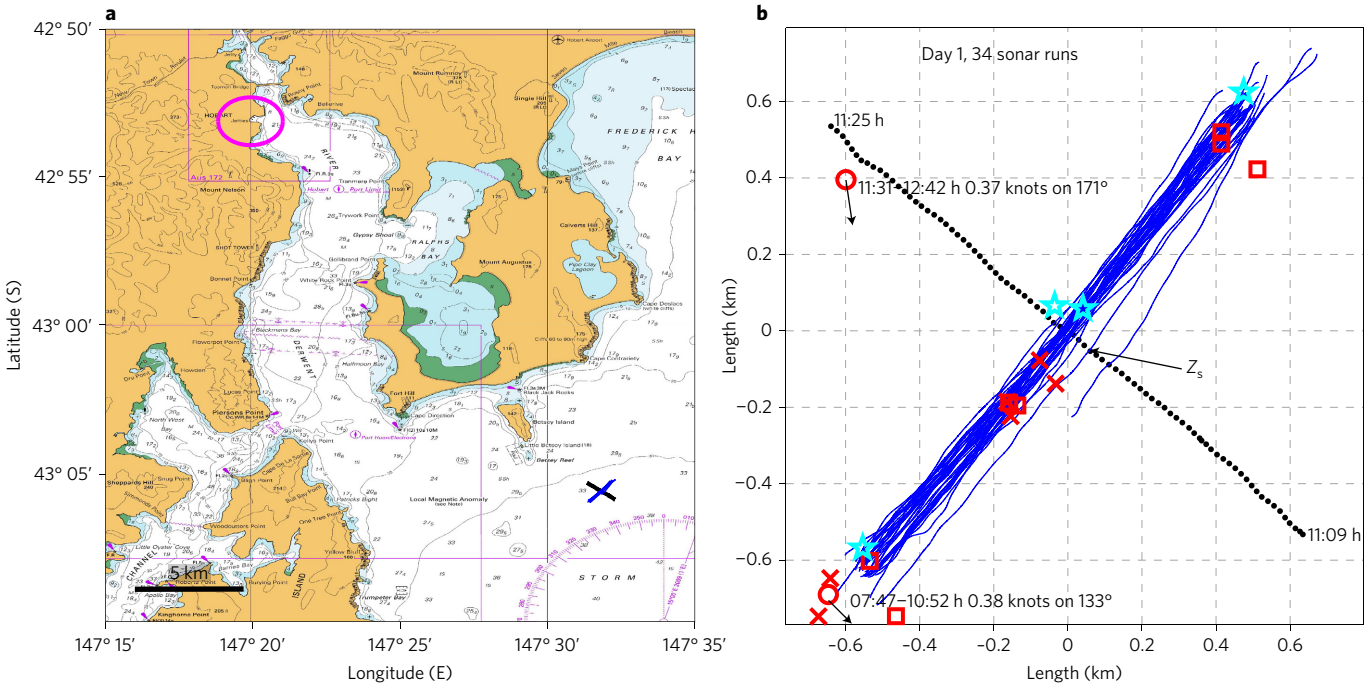

Figure 2 | Location of experimental site in southern Tasmania. a, General area showing air gun (black) and sonar transects (blue) overlaid on Australian chart AUS00796. The magenta circle is Hobart city (from Australian Hydrographic Service chart under Seafarer GeoTIFF Curtin University licence no. 2618SG). **b**, Close-up of experimental set-up for Day 1. Black dots, air gun signal locations; blue lines, sonar transects; red circles with arrows, drifters; red squares, control plankton tow locations; red crosses, plankton tow locations made after air gun exposure; cyan pentagrams, sea noise logger locations. One air gun sonar transect crossing point (Z_s) is shown. Axis scales are zeroed to the Z_e point. The world-wide location of the site was shown by the star in southern Tasmania in Fig. 1.

at 973–1,119 m, 795–932 m and 509–658 m (mean to median values using fitted power curves, $r^2 > 0.92$).

In addition to zooplankton abundance, mortality was assessed using vital stain counts and dead/total ratios (total being dead + live animals) as derived for taxonomic groups of copepods, nauplii and all other taxa (impact ranges and raw counts in Supplementary Tables 2 and 3, respectively). Vital stain control counts were pooled for each taxa per day. To look for range impact effects of air gun exposure in the vital stain results, exposed plankton tows were pooled into range groups of: (1) 79 m Day 1 + 71 m Day 1 + 149 m Day 2; (2) 451 m Day 1 + 547 m Day 2; and (3) 1,248–1,300 m Day 2 (Supplementary Table 3). There were significantly more dead animals in all taxa (copepods, nauplii and other taxa) for all range groups when comparing dead/total ratios of exposed with their respective controls (Fig. 3f for mean values, Supplementary Table 4 for statistics). In general, there were two to three times more dead zooplankton after air gun exposure compared with controls at all range groups for all taxa. All krill larvae found in all exposed samples were dead at all range groups following the air gun pass. The 'copepods dead' category was dominated by the smaller copepod species (*Acartia tranteri*, *Oithona* spp.). Although there were decreasing trends apparent in the ratio of dead to total counted with distance from impact for copepods and nauplii, these were not significant given the variance.

On Day 1, a 'hole' developed in the non-fish sonar backscatter (S_v) extending to ~20–30 m depth, which became noticeable 15 min after air gun passage and continued to expand and move coincident and symmetrically with the DTASL through time. When S_v in the upper 20 m of the water column was significantly reduced on Day 2, this 'hole' was not evident. Examples of the development of this 'hole' are shown in Fig. 4a–d, where consecutive sonar transects made every 15 min from the first air gun, sonar transect crossing time (T_{s1}), are shown.

To elaborate 'hole' definition, S_v on Day 1 was averaged over 6–16 m depth in 10 m range bins and is shown stacked in time zeroed to T_{s1} as a plan view in Fig. 4e along with the DTASL (noting the x axis here is time of full experiment, not distance). A noticeable drop in depth-averaged S_v can be seen in Fig. 4e 30 min post T_{s1} in the 6–16 m depth bin. In Fig. 4f, the average S_v over 6–16 m depth and for 100 m each side of the sonar and air gun line crossing point (Z_s) is shown, along with the average S_v for the same depth and range dimensions but following the DTASL for sonar transects after T_{s1}. A significant, 6 dB drop in depth-averaged S_v occurred 30 min post T_{s1} when following the DTASL track. A depth slice through the water column is shown in Fig. 4g, which averages S_v for five sonar pings either side of the Z_s point prior to air gun operations and which follows the DTASL trajectory for times after the start of air gun operations. The 'hole' in the plankton was clear down to 15 m depth appearing to extend as deep as 30 m, began to be noticeable in the 10–15 m depth range at 15 min post T_{s1}, was most persistent in the 10–13 m depth range and increased in radius through time.

The smoothed, depth- and range-averaged S_v curves for sonar transects after air gun crossing on Day 1 are shown in Fig. 5a, and the resulting 'hole' radius is shown increasing through time in Fig. 5b (see Methods). The development of the plankton backscatter 'hole' is clearly seen (sonar transects 27 onwards) in Fig. 5a, while the 'hole' radius increasing linearly with time is evident in Fig. 5b. The increase of the 'hole' radius through time gave a significant linear fit ($r^2 = 0.91$) with maximum radius based on the 3 dB drop (half power) below the least-impacted northeastern transect end, at 1,161 m, 78 min post T_{s1} during the last sonar transect, 34.

Passage of the operating air gun (Day 1) caused a 'hole' to open in sonar backscatter, a decrease in zooplankton abundance and increased dead/total zooplankton ratios in net tow observations. On Day 1, the sonar backscatter 'hole' followed the prevailing track of the air gun firing locations when these were corrected for water drift, was symmetrical about this track and showed a time-dependency, as evidenced by the 'hole' radius increasing for 78 min after the air

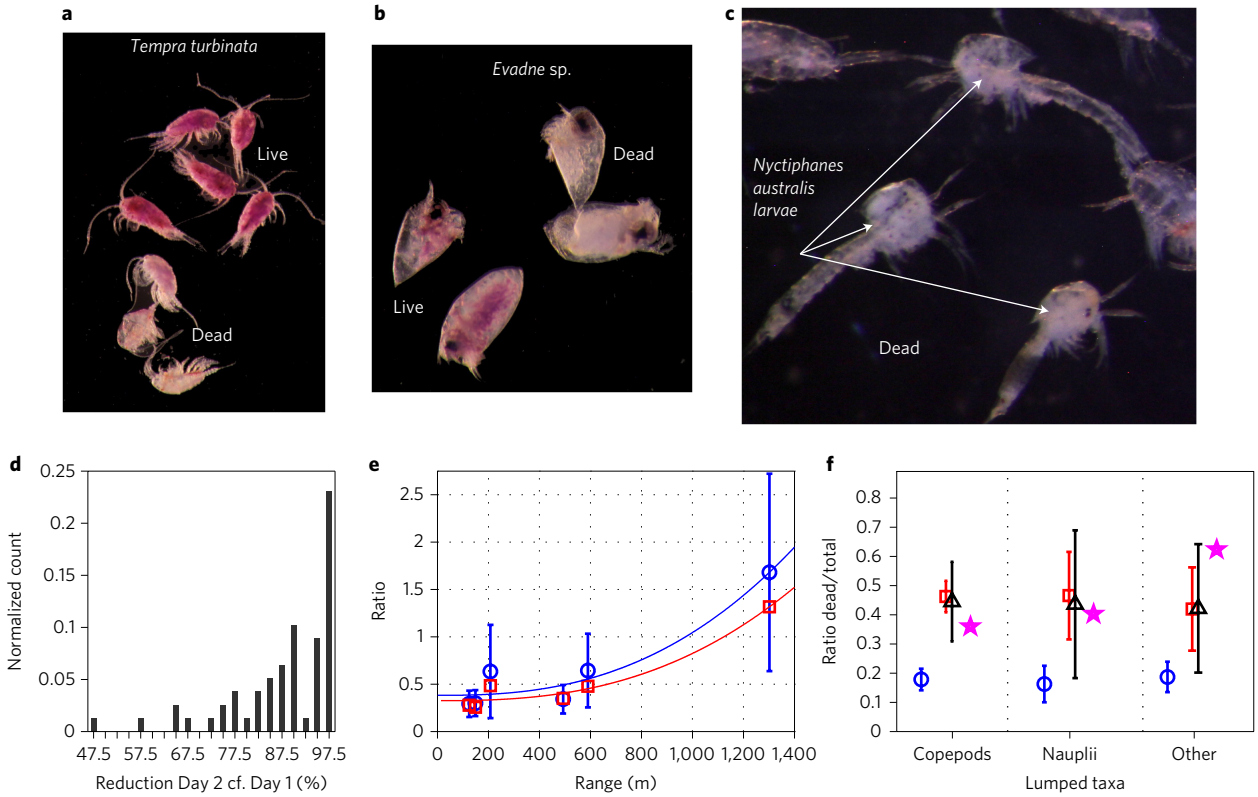

Figure 3 | Zooplankton vital staining images, and ratios of zooplankton abundance and dead to total plankton counted. a–c, Image of copepod (*Temora turbinata*, Temoridae; **a**), cladoceran (*Evadane* sp., Podanidae; **b**) and krill larvae (*Nyctiphanes australis*, Euphausiidae; **c**). **d**, Distribution for control samples of the percentage reduction in abundance of all net tows on Day 2 compared with Day 1. **e**, Ratio of exposed/control abundance for copepods and cladocerans with range from DTASL showing mean (circles), median (squares), and power fit to mean (blue) and median (red) values ($r^2 = 0.92$ and 0.96, respectively). **f**, Ratio of dead/total animals counted for copepods, nauplii and other zooplankton, with means of controls (blue circles), and 71–150 m (red squares), 451–547 m (black triangles) and 1,248 m (magenta stars) from DTASL. Error bars are 95% confidence limits. Live and dead animals are shown in the vital staining images.

gun crossed the sonar line. The maximum range for a reduction in sonar backscatter associated with the air gun impact track corresponded with the maximum sampling range for sonar (1.2 km). The lower zooplankton abundance on Day 2 meant the sonar backscatter 'hole' could not be visualized after air gun exposure, but like Day 1, on Day 2 statistically significant zooplankton mortality and decreased abundance were found after air gun passage. The zooplankton dead/total ratios were significantly reduced compared with controls at the maximum sampling range of ~ 1.2 km, although the abundance measures suggested a range for a detectable drop in abundance at approximately 1 km. Copepods and cladocerans had the greatest sample size for detecting range effects. Their abundance measures (ind. m^{-3}) after exposure had dropped to 50% of control abundance at 509–658 m from air gun passage, with no impact at 973–1,119 m (Fig. 3e). The received air gun level at 509–658 m range was 156 dB re 1 $\mu Pa^2\ s^{-1}$ sound exposure levels and 183 dB re 1 µPa peak-to-peak, and at 1.1–1.2 km range was 153 dB re 1 $\mu Pa^2\ s^{-1}$ and 178 dB re 1 µPa for the same units (Supplementary Fig. 2).

Discussion

On Day 2, even before the use of the air gun, the zooplankton net tow abundance counts were significantly lower than Day 1, and although individual fish sonar targets were of similar abundance, there was a significant increase in fish presence higher in the water column. The drop of zooplankton abundance on Day 2 compared with Day 1 and increase of fish in the water column on Day 2 raises the question of whether the scale of air gun impact on Day 1 carried over into Day 2. The tidal regime was oscillatory (diurnal tide; Supplementary Fig. 3) and sampling was approximately 24 h apart, but the impact range measured (1.2 km) was unlikely to have been large enough to overcome mixing or advection. Without detailed information on mixing, advection and current set above tidal flow (not known), it is not possible to draw any conclusions on the difference of zooplankton abundance and fish depth observed between Days 1 and 2.

Previous attempts to quantify ecological scale impacts on planktonic larvae from seismic surveys used modelling scenarios with impact ranges of <10 m (refs [14,15]) and suggested insignificant impacts compared with the naturally high turnover of plankton[25]. The impact range observed here, at the maximum range sampled of 1–1.2 km, is more than two orders of magnitude higher than what was assumed in these modelling studies. The impacts seen here were taxon-, range- and time-dependant, with outside bounds for time (1.2 h) and range impacts on the maximum scale of sampling.

Although we did not study the impact mechanism of the impulsive air gun signal, we can present a hypothesis on what may have occurred. Many marine invertebrates, late stage larval fauna and the zooplankton Mysidae use mechanoreceptors of a small, dense mass to 'drive' sensory hairs ('statocyst' systems[26]) partly for vibration perception. Most zooplankton do not have mass loaded mechanosensory systems but have external sensory hairs on the distal antenna ends, attached to 'rigid and stiff' sections of cuticle[27,28], with the cuticle potentially acting as a mechanical impedance for the sensory hairs to move against when driven by hydrodynamic stimuli. The zooplankton mechanosensory systems may by extremely sensitive[29] and either system will respond to an impulsive air gun signal by

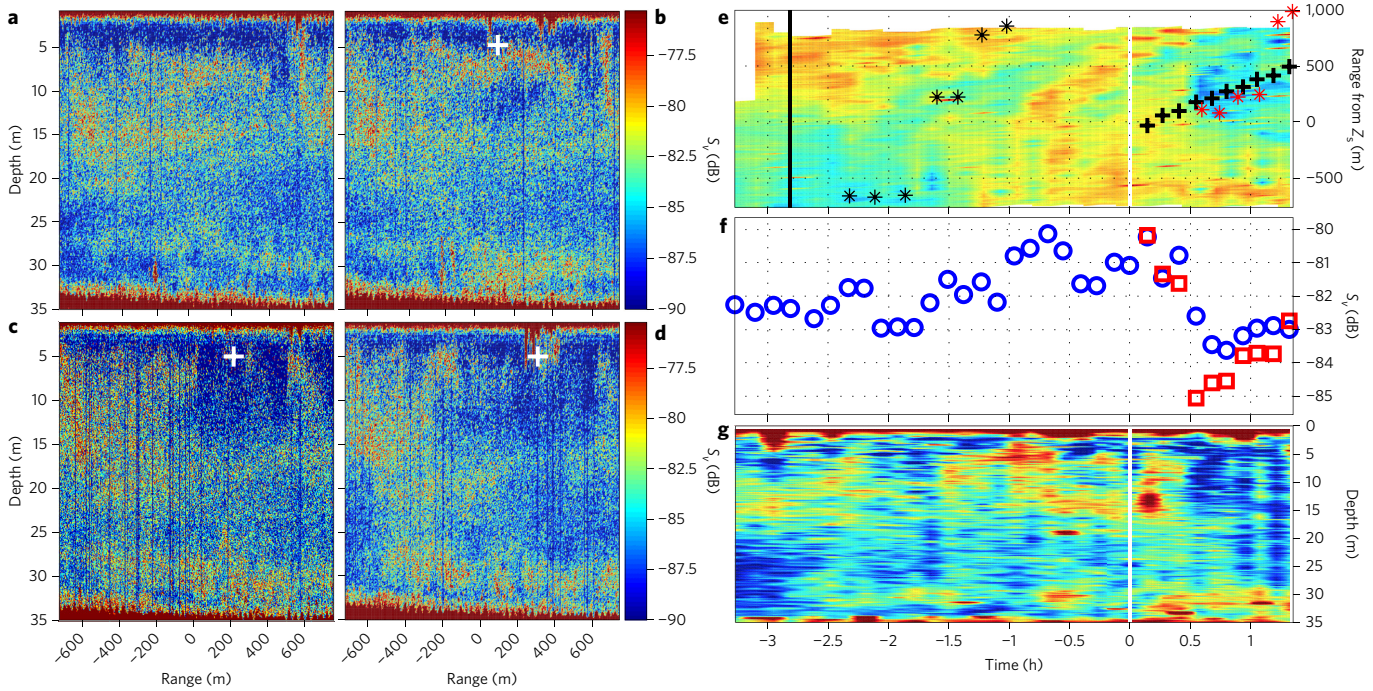

Figure 4 | S_v after Day 1 air gun exposure. a, Immediately before air gun crossing sonar line (run 25). **b**, 15 min after air gun crossed sonar line (run 27). **c**, 32 min after air gun crossed sonar line (run 29). **d**, 47 min after air gun crossed sonar line (run 31). **e**, Plan view of Day 1 range and depth-averaged S_v with range from Z_s (air gun/sonar crossing point) as *y* axis and time from T_{s1} (white line) as *x* axis. **f**, Averaged S_v from 100 m each side of Z_s over 6–16 m depth (circles) with red squares centred on DTASL (drifted location of air gun signal that most impacted sonar line). **g**, A vertical slice through the water column averaged five pings either side of Z_s before air gun crossing then DTASL after air gun starts. The white crosses in **b**–**d** represent DTASLs, as do black crosses in **e**; the vertical black line in **e** is time of control air gun pass, black asterisks show control plankton tow locations and red asterisks show exposed plankton tow locations. The axes and colour scales are matched in **a**–**d**, and **e** and **f**. Range in **a**–**d** is from Z_s.

'shaking', hypothetically, to the point where damage could accrue to sensory hairs or tissue. A subsequent loss or degradation of sensory ability would explain differing results among zooplankton taxa, as there are vast differences in presence, morphology and sensitivity of such systems. Impacted animals might not die immediately after air gun exposure, but rather may be disabled in their sensory capacity with an accompanying loss of fitness and so increased predation risk through time. An orientation disability would alter observed sonar reflectivity as swimming orientations changed from the upright position. The 120 kHz sonar frequency used in experiments will not observe individual zooplankton directly but will measure reflectivity from aggregated zooplankton, thus the observed 'hole' may have been due to a statistical change in zooplankton orientation or to dispersal of aggregations.

Plankton lie well on the *r* side of the *r*/*K* continuum in life strategies[1]. *r*-selected species typically have a short life span, large numbers of offspring and little if any offspring care, whereas *K*-selected species have the reverse. For anthropogenic sources to have significant impacts on an ecological scale on plankton, then the spatial or temporal scale of impact must be large in comparison with the ecosystem concerned. More than 90% of seismic surveys are conducted in a three-dimensional (3D) mode, where the density of sampling points allows 3D imaging of sub-sea geology[5]. These 3D surveys are focussed from a few hundred to thousands of square kilometres, taking weeks to months to complete, and importantly have repetitive signal locations well within the impact ranges observed here (15–25 m along line, 400–800 m across line[5]). Given the extensive spatial scale for serious impacts on plankton observed here, combined with the repeat and sustained nature of many seismic surveys in a comparatively small spatial area, it is highly probable that significant depletion or modification of plankton community structure is occurring on the scale of 3D seismic surveys undertaken.

The significance and implications of potential large-scale modification of plankton community structure and abundance due to seismic survey operations has enormous ramifications for larval recruitment processes, all higher order predators and ocean health in general. There is an urgent need to conduct further study to mitigate, model and understand potential impacts on plankton and the marine environment, and to prioritize development and testing of alternative seismic sources.

Methods

Summary. Two replicated experiments were carried out in Storm Bay at the southeastern end of Tasmania, Australia, at the same location across a uniform 34–36 m depth seabed (Figs 1 and 2) on 2 and 3 March 2015 (Days 1 and 2). Each experiment involved: (1) deployment of acoustic noise loggers with surface buoys at the extremities (1.6 km apart) and centre of a planned line of sonar transects (planned zero point for experiment, or Z_e) to measure air gun signals; (2) deployment of a drifter with drogue at 5 m depth to track surface water drift; (3) CTD measures (Day 2); (4) a control air gun transect, with the air gun (2.46 l or 150 inch^3 volume) deployed, the source vessel run on a heading perpendicular to and starting 800 m from the sonar transect, through the Z_e out to 800 m past, but the air gun not operated (1.6 km air gun line); (5) replicate control vertical plankton tows at nominally 0, 250 and 800 m southwest of the Z_e from the seabed to surface using a bongo net with two 0.75 m mouth diameter, 200 µm nets with flow meter and samples split into formalin and a vital stain (so two plankton tows at each nominal range, two cod-ends per tow, to give 12 cod-ends each day at a mean net ascent rate of 0.25 m s^{-1}); (6) active air gun transect (location and headings identical to control); (7) replicate vertical plankton tows after completion of the air gun transect (sampling same as controls); and (8) continual sonar observations between the buoys marking the sonar transect end points. Sonar transects were made for ~3 and 1.5 h pre- and post- the active air gun passage, respectively. Weather was calm on Day 1 (<12 knots) and calm to moderate on Day 2 (12–18 knots). Details of control and active air gun transects and sonar transects are listed in Supplementary Table 5. Note that the actual air gun and sonar transects did not exactly cross through the planned experimental zero point (Z_e), thus the crossing location of each sonar and air gun transect for that day is termed the point Z_s, which is unique for each sonar transect. The measured water

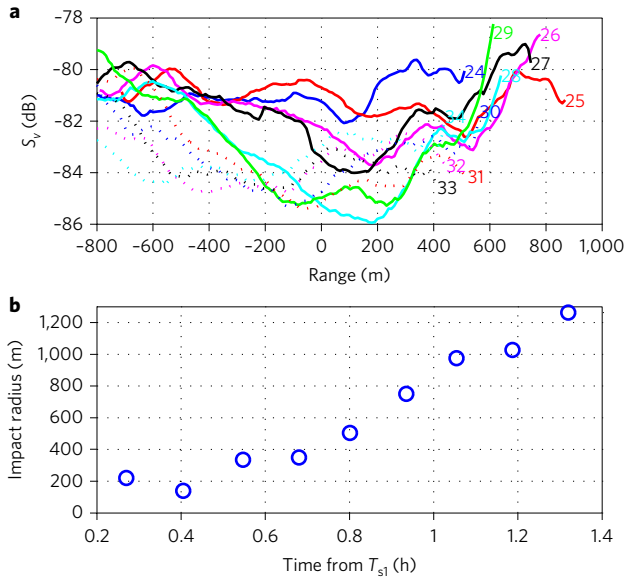

Figure 5 | Quantification of S_v hole averaged within 10–12.5 m depth range. a, Smoothed, averaged S_v on Day 1 for sonar transects 24–34 after the air gun had crossed the sonar transect (that is, from and inclusive of T_{s1}, which occurred during sonar transect 24). The sonar transect numbers are shown for each curve (transects 24-29 solid lines, 30-34 dotted lines) and the and the zero range point is the DTASL (drifted location of air gun signal that most impacted that sonar line). **b**, The measured radius of impact for the zooplankton 'hole', symmetric about the DTASL as given by 3 dB down points below the mean of the first 90 m from the northeast (−ve), plotted with time from T_{s1}, is shown. Note that many sonar transects extended beyond the −800 m shown.

body drift direction and rate was used to account for water impacted by the air gun signals, which when it was sampled by plankton tow or sonar, had drifted (termed DTASL, see below).

Air gun operations. A Sercel G. Gun II with a 2.46 l (150 cubic inch) chamber was used as the air gun source, towed at 5.1 m depth 17 m astern the 11 m vessel FV *Shelle Ton* (10 t gross, 400 hp single propeller). Two GPS units logging every 1 s were mounted side-by-side inboard with the aerial and tow offsets used to calculate air gun location. A near-field hydrophone (HTIU-90) was located 0.5 m off the gun ports and all near-field air gun signals logged to a Sound Devices (SD) 722 or 744 digital recorder, using a −20 dB pre-amplifier, −5 dB gain on the recorder and 24 bit, 48 kHz sampling. The time of the first shot was logged manually and the SD logged near-field hydrophone, air gun signal times used to define all shot fired times. These fired shot times were used to interpolate into the source vessel navigation data to derive the fired signal location. The air gun was operated from a bank of four G-size high-pressure air bottles (35 MPa or 350 bar). Twin SCUBA compressors were operated in parallel to pump the bottles. Approximately 110 shots at full pressure (13.8 MPa or 2,000 psi) were available with full gas bottles and the compressors running. All air gun signals were at 13.8 MPa (2,000 psi). Four vessel crew were used, a skipper, marine mammal observer and two air gun operators.

CTD casts. A Seabird SBE19plus CTD profiler was used on Day 2, with one cast pre-exposure and one post-exposure, each within 100 m of the Z_s point. Data were read and plotted (Supplementary Fig. 1) to ascertain if the water column was well mixed or stratified.

Drifter deployments. Two deployments of a drifter were made on Day 1 and one on Day 2. The drifter comprised a sea anchor (drogue) of 1 m diameter attached to a weighted line at 5 m depth. A surface buoy and a buoy with pole and flag were attached at the surface. The universal time and GPS position of deployment, during deployment and recovery locations were logged.

Water body drift allowance. All plankton net tows and sonar transects were made along approximately the same line perpendicular to the centre of the air gun transect (Z_s point). Many of the sonar transects and plankton tows were made after air gun operations commenced or ceased. The water body was drifting. Thus for sonar transects or plankton tows after air gun operations commenced, allowance had to be made for water drift moving the air-gun-impacted water body, to ascertain the nearest location of the water body impacted by a fired air gun signal for that sampling time point (plankton tows) or time period (sonar transect). To account for drift of the air-gun-impacted water body during sonar transects sampled after air gun operations commenced, several steps were required. First, the location of all air gun signals fired before a sonar ping time point were displaced in the water body drift direction for the distance given by the water body drift rate and elapsed time between that sonar ping and air gun firing. The air-gun-signal-displaced location that had the minimum range difference to the sonar ping location gave the displaced air gun signal location for that sonar ping. This was iterated for all sonar pings in a sonar transect, and the minimum range of the displaced air gun signal locations to all sonar pings in the transect gave the air gun signal location that most impacted that sonar transect. This location has been termed the drift translated air gun signal location (DTASL) and applies to a sonar transect. An example of the air gun signal displacement accounting for drift for the ping at which the DTASL occurred on sonar transect 30, Day 1, is shown in Supplementary Fig. 4. The similarly derived air-gun-displaced location, accounting for drift and time (sampling time minus air gun fire time), that best matched the plankton net tow location, gave the range of plankton net tow to air gun shot firing point, with these ranges listed in Supplementary Table 2.

Sonar. Sonar transects were made using a Simrad EK60 echosounder mounted on a pole bolted athwartships a 6 m vessel. A single beam, 120 kHz transducer was mounted at 0.5 m depth, using a 156 ms ping rate, maximum power, pulse length of 0.06–1.02 ms (depth resolution of 0.048 m) with a mean vessel speed of 3.2 ± 0.10 m s^{-1} (or 6.4 ± 0.21 knots) and median time for a line 8.2 min. On Day 1, 34 sonar transects were completed, 23 before the active air gun transect, 3 during and 8 after. On Day 2, 28 sonar transects were completed, 19 before the active air gun line, 4 during and 5 after. Details of sonar transects are listed in Supplementary Table 5.

The sonar data raw files were read into MATLAB (Mathworks) and converted to grids of calibrated volume backscattering strength (S_v in units of dB m^{-3}) with associated navigation and time data. The sonar navigation data were used to align each sonar transect, deemed to be from one end of its line to the other before or after turns, to the crossing point of the active air gun track for that day. The air gun crossing point was set as the zero range location for that transect (the air gun track was interpolated at a 1 m resolution and the closest sonar ping location to the air gun track found and deemed to be the zero point for that sonar transect, Z_s). Each ping along a sonar line was assigned a range perpendicular to the Z_s point and its sign set so that the northeastern portion of the line was −ve and the southwestern portion +ve. Each sonar transect had a start time, end time and air-gun-line crossing time (T_s). The difference between T_s and the first sonar transect crossing time, T_{s1}, gave the time the sonar transect preceded (−ve) or followed (+ve) the time the air gun crossed the first sonar transect.

The 120 kHz S_v values have been averaged in different range and depth bins. All S_v averaging was carried out in the linear domain ($L = 10^{(S_v/10)}$, where L is the linear value of S_v), summed as appropriate then divided by the number of depth bins and pings, and the result converted back to decibels ($10 \times \log_{10}(L)$). All zooplankton S_v averaging had the surface bubble layer, fish schools, individual fish targets and bad pings removed before averaging. The surface bubble layer was found by following a ping down from the surface in consecutive 3 m bins and finding the first bin with no S_v values exceeding −68 dB. The start of the next bin + 1 m was taken as the surface depth free of surface bubble contamination. Individual fish targets were found by locating the characteristic chevron shape of a fish backscatter return as it moved through the sonar beam. The dimensions of these targets, plus surrounding pings out to 0.25 m, were removed from all analysis of mean S_v values. There were several fish schools on each day; these could not be resolved as individual targets so the boundary of each school was established manually and the schools removed from all analysis of mean S_v values. Several sonar pings were artificially low, usually due to high attenuation of the signal in the surface bubble layer. These pings were found by deriving the median value from below the surface bubble layer to just above the seabed for each ping, and removing any pings where the median value was <−95 dB. These 'bad pings' were excluded from all analyses.

The development and dimensions of the sonar backscatter 'hole' that developed post air gun passage on Day 1 were quantified by averaging S_v in the depth of maximum impact over 10–12.5 m in 10 m range bins along a sonar line, smoothing the resulting curve using a running linear fit (8 points either side), calculating the range at which the curve fell 3 dB (half power) below the mean S_v calculated over 90 m from the northeastern line end (least impacted end of sonar due to prevailing drift), and where possible finding the 3 dB down-crossing points symmetric about the DTASL. On Day 1, when moving from −ve to +ve ranges (northeast to southwest), the curve always fell below the threshold leading towards the DTASL as the drift was taking the water mass in the +ve direction, but the curve did not necessarily climb back up to this value on the southwestern side of the DTASL, as the sonar transects were too short at the longer time periods post T_{s1}. Where the curve did cross the threshold on the northeast and southeast side of the DTASL, the difference in range values at each threshold was divided by two to give the radius of the 'hole', where the curve did not reach the threshold on the southeastern side (transects 31–34), the radius was derived as the distance of range at the

DTASL minus distance of where the curve reached the 3 dB down-threshold on the northeastern side.

Air gun signal measures. Three sea noise loggers were set on the seabed during each day's experiment, one in the centre of the air gun transect (a) and two at the ends of the sonar transects (b and c). A fourth sea noise logger (d), with hydrophone located 9.4 m below the sea surface, was suspended from surface floats above receiver (a). All sea noise loggers recorded pressure while (b) and (c) also recorded ground-borne vibration via geophones. The sea noise loggers were Curtin University designed, CMST-DSTO sea noise recorders (see www.cmst.curtin.edu.au/products). The two noise loggers at the centre of the air gun line (a and d) sampled 2 channels at 0 and 20 dB gain (50 min of every hour at 4 kHz sample rate) with the low gain channel not overloading for air gun signals at short range. The noise loggers at the sonar line ends used 20 dB gain and 4 kHz sample rate (2,600 s every hour) with no overloading of air gun signals. All noise loggers had a High Tek HTI U90 hydrophone, individually calibrated with sensitivities ranging from −197.6 to −197 dB re 1 V μPa^{-1}. All air gun lines were carried out during the 'on' times of all receivers. All sea noise recorders were calibrated for the pressure response by inputting white noise of known level into the instrument with the white noise and hydrophone in series. Analysis of the logged signal gave the system gain with frequency, accounting correctly for the impedance match of the hydrophone, pre-amplifier and system electronics. This system gain curve was used with the known hydrophone sensitivity to convert the logged volts to pascals in the time domain with the system response calibrated over 1 Hz to the anti-aliasing filter frequency. The on-board noise logger clocks were set to GPS, universal time transmitted before deployments and the drift read after recovery to give absolute timing accuracies of <0.1 s.

Air gun signals were analysed as described in ref. [24], briefly by: (1) extracting the signals from the sea noise logger files; (2) converting volts to sound pressure (Pa) using the system calibration curve (system gain with frequency) and hydrophone sensitivity in the time domain; (3) characterizing the air gun signal for 16 signal parameters as defined in ref. [30]; and (4) aligning the shot received time with source navigation data to give source–receiver slant range (direct path source to receiver). The signal parameters of sound exposure levels and peak-to-peak have been used here to describe air gun signal levels. Sound exposure levels were calculated as in ref. [30].

Plankton tows and analysis. At each site, the first tow cod-ends (two of) were placed into the vital stain neutral red, the second tow had one cod-end into neutral red and the second into 4% buffered formaldehyde. The GPS time and co-ordinates of each drop (1: start lowering; 2: reach bottom and start raising; and 3: at surface) were made by a dedicated observer, as were the flow meter readings (model GeoEnvironmental, serial no. 23227) before and at the end of each tow. The summary vertical ascent times, rates, the horizontal distance moved during ascent and the volume sampled by each cod-end using the GPS distance traversed, water depth and net radius are listed in Supplementary Table 6. The water volume sampled during each tow was calculated using the GPS data from the horizontal drift (GPS) and water depth (sonar) to give distance of the net tow, which combined with the area of the net mouth opening gave volume of water sampled for each cod-end and therefore net. The flow meter readings were calibrated to cubic metres of water sampled, but while many agreed with the GPS calculations, some were less than as derived from the net radius and water depth. The flow meter used was capable of spinning backwards, possibly during descent, thus in abundance analysis the GPS-derived water volume sampled by each tow was used.

Samples of zooplankton that had been preserved in formaldehyde were identified and counted using a Leica M165C stereomicroscope. Where necessary, samples were split with a Folsom plankton splitter[31], until there were between 500 and 1,000 individuals in a subsample. All zooplankton in each subsample were identified to the lowest taxonomic level possible; genus or species level for copepods, cladocerans, chaetognaths and euphausiids, and higher levels for other groups.

The methods used for assessing plankton survival followed that of ref. [32]. Vital stained samples were frozen after collection in the field, thawed individually in cold, filtered (0.2 µm) seawater, acidified with a small volume (~1 ml) of 1 M HCl, rinsed with small amounts of filtered seawater, subsampled so that >400 individuals were counted (three replicates each sample) and backwashed into a sorting tray. The samples were examined under a Leica M165C stereomicroscope, fitted with a Canon 5D Mark II camera. Samples were examined using dark field microscopy, which maximized the contrast between live (bright pink after having taken up the vital stain internally) and dead (pale pink, having not taken up the stain internally) specimens. Processing of each sample was completed within 60 min, as after that time the sample became visibly degraded. The ratio of dead zooplankton to total numbers of that taxa counted were derived for each tow.

In assessing change in abundance of zooplankton between pre-air-gun periods on Day 1 compared with Day 2 or control versus exposed periods on Day 1 and Day 2, counts of ind. m^{-3} have been compared as ratios and two-tailed *t*-tests used to determine if the sets of ratios differ. Comparisons were made for control tows of Day 2 divided by control tows of Day 1 abundance to determine how the site differed between days, or of exposed divided by mean control abundance (exposed/control), including data from both days, to compare how air gun exposure impacted measured abundance. As there is normally naturally high spatial variability in plankton abundance, and as there was a time offset between control and exposed plankton tows, then for calculation of exposed divided by mean control abundance, daily control abundance was averaged within a taxa (that is, the mean of the control abundance values at the three nominal ranges that day was used). Control abundance variability ratios were calculated for all combinations of non-zero plankton tows within a taxa and day, and combined for appropriate taxa to compare with exposed divided by mean control ratios. Any taxa with zero control or exposed counts was excluded, leaving 189 taxa/tow combinations ('taxa/tow') for comparison. The ratios of exposed divided by control abundance have been expressed as percentage reductions, or [1-Ratio] × 100. To compare abundance trends for taxa with range, drift-corrected impact ranges were used and power curves of the form $y = a \times x^b + c$ fitted to data, where y is ratio exposed/control abundance, x is range (m), and a, b and c are fitted constants. Correlation coefficients were calculated for all fits.

General analysis. All air gun, sonar and spatial analysis was carried out in the MATLAB (Mathworks) environment using purpose-built software. All times given are Australian eastern standard time daylight saving, or universal time + 11 h. Errors given against mean values are indicated as ±95% confidence intervals or standard deviation as s.d. Samples sizes are given as *N*.

Data availability. The sonar data that support the findings of this study are available on request from the corresponding author, while the zooplankton abundance and vital staining results are available in the Supplementary Information.

Received 4 October 2016; accepted 16 May 2017; published 22 June 2017

References

1. Alcaraz, M. & Calbet, A. *Zooplankton Ecology* (Encyclopedia of Life Support Systems, 2009).
2. Raymont, J. E. G. *Plankton and Productivity in the Oceans* Vol. 2 (Pergamon, 1983).
3. Richardson, A. J. In hot water: zooplankton and climate change. *ICES J. Mar. Sci.* **65,** 279–295 (2008).
4. U.S. Geological Survey World Conventional Resources Assessment Team *Supporting Data for the U.S. Geological Survey 2012 World Assessment of Undiscovered Oil and Gas Resources U.S. Geological Survey Digital Data Series DDS–69–FF* (USGS, 2013); http://pubs.usgs.gov/dds/dds-069/dds-069-ff/
5. *An Overview of Marine Seismic Operations* Report 448 (OGP and IAGC, 2011); http://www.iogp.org/bookstore/product/an-overview-of-marine-seismic-operations/
6. *Industry Statistics* (APPEA, 2016); http://www.appea.com.au/industry-in-depth/industry-statistics/
7. Ivanova, A. *et al.* Monitoring and volumetric estimation of injected CO_2 using 4D seismic, petrophysical data, core measurements and well logging: a case study at Ketzin, Germany. *Geophys. Prospect.* **60,** 957–973 (2012).
8. Richardson, W. J., Greene, C. R., Malme, C. I. & Tomson, D. H. *Marine Mammals and Noise* (Academic, 1995).
9. Popper, A. N. & Hastings, M. C. The effects on fish of human-generated (anthropogenic) sound. *Integr. Zool.* **4,** 43–52 (2009).
10. Pearson, W. H., Skalski, J. R. & Malme, C. I. Effects of sounds from a geophysical survey device on behaviour of captive rockfish (*Sebastes* spp.). *Can. J. Fish. Aquat. Sci.* **49,** 1343–1356 (1992).
11. Fewtrell, J. L. & McCauley, R. D. Impact of airgun noise on the behaviour of marine fish and squid. *Mar. Pollut. Bull.* **64,** 984–993 (2012).
12. Neo, Y. Y. *et al.* Impulsive sounds change European seabass swimming patterns: influence of pulse repetition interval. *Mar. Pollut. Bull.* **97,** 111–117 (2015).
13. McCauley, R. D., Fewtrell, J. & Popper, A. N. High intensity anthropogenic sound damages fish ears. *J. Acoust. Soc. Am.* **113,** 638–642 (2003).
14. Kostyuchenko, L. P. Effects of elastic waves generated in marine seismic prospecting on fish eggs in the Black Sea. *Hydrobiol. J.* **9,** 45–48 (1971)
15. Dalen, J. & Knutsen, G. M. in *Progress in Underwater Acoustics* (ed. Merklinger, H. M.) 93–102 (Plenum, 1986).
16. Hawkins, A. D. Pembroke, A. E. & Popper, A. N. Information gaps in understanding the effects of noise on fishes and invertebrates. *Rev. Fish. Biol. Fish.* **25,** 39–64 (2015).
17. Day, R. D., McCauley, R. D., Fitzgibbon, Q. P. & Semmens, J. M. *Assessing the Impact of Marine Seismic Surveys on Southeast Australian Scallop and Lobster Fisheries Final Report* 2012-008-DLD (FRDC, 2016); http://frdc.com.au/research/final-reports/Pages/2012-008-DLD.aspx
18. de Soto, N. A. *et al.* Anthropogenic noise causes body malformations and delays development in marine larvae. *Sci. Rep.* **3,** 2831 (2013).

19. Day, R. D. *et al.* Seismic air gun exposure during early-stage embryonic development does not negatively affect spiny lobster *Jasus edwardsii* larvae (Decapoda: Palinuridae). *Sci. Rep.* **6,** 22723 (2016).
20. Yen J., Rasberry, K. D. & Webster, D. R. Quantifying copepod kinematics in a laboratory turbulence apparatus. *J. Mar. Syst.* **69,** 283–294 (2008).
21. McManus, M. A. & Woodson, C. B. Plankton distribution and ocean dispersal. *J. Exp. Biol.* **215,** 1008–1016 (2012).
22. Bianco, G. *et al.* Analysis of self-overlap reveals trade-offs in plankton swimming trajectories. *J. R. Soc. Interface* **11,** 20140164 (2014).
23. Visser, A. W. Motility of zooplankton: fitness, foraging and predation. *J. Plank. Res.* **29,** 447–461 (2007).
24. McCauley, R. D., Duncan, A. J., Gavrilov, A. N. & Cato, D. H. Transmission of marine seismic survey, air gun array signals in Australian waters. In *Proc. ACOUSTICS 2016* (eds Hillock, I. D. M. & Mee, D. J.) 1–10 (Acoustics Australia, 2016).
25. McCauley, R. D. in *Environmental Implications of Offshore Oil and Gas Development in Australia: The Findings of an Independent Scientific Review* (eds Swan, J. M., Neff, J. M. & Young P. C.) 19–122 (APPEA, 1994).
26. Budelmann, B. B. in *The Evolutionary Biology of Hearing: Hearing in Nonarthropod Invertebrates* (eds Webster, D. B. *et al.*) Ch. 10, 141–155 (Springer, 1992).
27. Lenz, P. H., Weatherby, T. M., Weber, W. & Wong, K. K. Sensory specialization along the first antenna of a calanoid copepod, *Pleuromamma xiphias* (Crustacea). *Mar. Freshw. Behav. Physiol.* **27,** 213–221 (1996).
28. Weatherby, T. M. & Lenz, P. H. Mechanoreceptors in calanoid copepods: designed for high sensitivity. *Arthropod Struct. Dev.* **29,** 275–288 (2000).
29. Buskey, E. J., Lenz, P. H. & Hartline, D. K. Sensory perception, neurobiology, and behavioral adaptations for predator avoidance in planktonic copepods. *Adapt. Behav.* **20,** 57–66 (2011).
30. McCauley, R. D. *et al.* in *Environmental Implications of Offshore Oil and Gas Development in Australia: Further Research* 364–521 (APPEA, 2003).
31. Motoda, S. Devices of simple plankton apparatus. *Mem. Fac. Fish. Hokkaido Univ.* **7,** 73–94 (1959).
32. Elliott, D. T. & Tang, K. W. Simple staining method for differentiating live and dead marine zooplankton in field samples. *Limnol. Oceanogr. Meth.* **7,** 585–594 (2009).

Acknowledgements

The authors acknowledge the fieldwork contributions of IMAS staff, particularly M. Porteus, L. Watson, J. Beard, A. Pender, J. McAllister and A. Walters. M. Perry and D. Minchin of Curtin University prepared air gun and acoustic gear. This study was supported by University of Tasmania Research Enhancement Grant Scheme D0022818. R.A.W. acknowledges support from the Australian Research Council (Discovery project DP140101377). All research was conducted in accordance with University of Tasmania Animal Ethics Committee permit A13328. Fieldwork was conducted in accordance with Tasmania Department of Primary Industries, Parks, Water and Environment permits 13011 and 14038. R. Towler (Midwater Assessment and Conservation Engineering, NOAA Alaska Fisheries Science Center) produced a modified package for reading the sonar raw data files into MATLAB.

Author contributions

R.D.M., R.D.D., Q.P.F. and J.M.S. conceived the study, with R.D.M. setting the initial study plan based on previous experiences. All authors but R.A.W. contributed to the final study design and field planning. R.D.M. and R.D.D. collected field data. K.M.S. and R.D.D. analysed plankton tows. R.D.M. analysed air gun and sonar data, and wrote the main manuscript. All authors reviewed and revised the manuscript.

Additional information

Supplementary information is available for this paper.

Reprints and permissions information is available at www.nature.com/reprints.

Correspondence and requests for materials should be addressed to R.D.M. and J.M.S.

How to cite this article: McCauley, R. D. *et al.* Widely used marine seismic survey air gun operations negatively impact zooplankton. *Nat. Ecol. Evol.* **1,** 0195 (2017).

Publisher's note: Springer Nature remains neutral with regard to jurisdictional claims in published maps and institutional affiliations.

Competing interests

The authors declare no competing financial interests.